

## Nano Structural Properties of Lead Doped Cadmium Sulfide ( $Cd_{1-x}Pb_xS$ ) Thin Films Deposited by Spray Pyrolysis Technique

Ranojit Kumar Dutta<sup>a, b and c</sup>

<sup>a</sup>Assistant Professor, Faculty of Science and Engineering, City University, Dhaka 1216, Bangladesh

<sup>b</sup>Department of Physics, Faculty of Engineering, Bangladesh University of Engineering and Technology (BUET), Dhaka 1000, Bangladesh.

<sup>c</sup>Researcher, College of Hydraulic & Environmental Engineering, China Three Gorges University, Yichang, 443002, Hubei, P.R.China.

ranojit.dutta83@gmail.com

### Abstract

Lead doped cadmium sulfide thin films  $Cd_{1-x}Pb_xS$  ( $0 \leq x \leq 0.20$ ) were deposited onto a glass substrate at a temperature of 523K at a low-cost spray pyrolysis technique. They were characterized by their structural and optical properties, by energy dispersive x-ray analysis, scanning electron microscopy, x-ray diffraction respectively. X-ray diffraction patterns of the films are identified as (100), (002), (101), (102), (110), (103) and (201) planes which have hexagonal crystal structure. No extra peak developing with the increasing Pd concentration. The direct band gap energy of the film depends on the concentration. This value varies from 2.52 eV to 2.17 eV as required for solar cell and opto-electronic device applications.

**Keywords:** Nano Structural Properties, Optical Properties, Spray Pyrolysis, Cds And Pbs, Semiconductors.

### 1. Introduction

CdS and PbS are sensitive to light. Based on their practical application, a study of their mixed thin film structure as spray pyrolysis converters is of technical importance [1]. For the preparation CdS and Pb doped CdS thin films, a variety of deposition techniques, including Chemical Bath Deposition technique (CBD) [2-6], aqueous synthesis [7, 8], precipitation technique [9, 10] and quenching method [11] have been used. Spray pyrolysis deposition technique has been a viable technique to produce  $Cd_{1-x}Pb_xS$  films because it several advantages such as low cost experimental set up, high spatial selectivity, precise control over maneuvering the impurity concentration and possibility to overcome the solubility limit [1, 12-16].

The present paper aims to investigate the optical band gap prepared by lead doped cadmium sulfide thin films deposited onto a glass substrate at a temperature of 523K using a cost-effective spray pyrolysis technique.

### 2. Material and Methods

#### 2.1 Experimental details

Lead doped cadmium sulfide thin films  $Cd_{1-x}Pb_xS$  ( $0 \leq x \leq 0.20$ ) were prepared using a low cost spray pyrolysis technique. Aqueous solution of 0.1M cadmium acetate, Cd ( $CH_3COO$ )<sub>2</sub>.3H<sub>2</sub>O, 0.2M thiourea (NH<sub>2</sub>CSNH<sub>2</sub>) and 0.1M lead acetate, Pb(CH<sub>3</sub> COO)<sub>2</sub> .2H<sub>2</sub>O were taken as sources of Cd, S and Pb respectively. A considerable amount of (100 ml) solution was taken in the Beaker. The clean substrate (5cm×2cm) with a suitable mask was put on the susceptor of the heater. The distance between the tip of the nozzle and the surface of the glass substrate was kept at 25 cm. The substrate temperature was measured by placing a copper constantan thermocouple. Thin film condensation involves three distinguished mechanisms depending on the strength of interaction among the atoms of the growing film and that among the atoms of the film and substrate.

### 3. Results and Discussion

#### 3.1. Structural properties

X-ray diffraction patterns of the films are shown in Figure 1. Some peaks, identified as (100), (002), (101), (102), (110), (103) and (201) planes, matched the standard (JCPDS data card 41-1049,  $a=4.140\text{\AA}$  and  $c=4.140\text{\AA}$ ) of CdS hexagonal crystal structure. No extra peak developing occurs when Pd concentration increases. The lattice parameters were estimated for (100) and (002) planes using the relation (1)

$$\frac{1}{d_{hkl}} = \left[ \frac{4}{3} \frac{(h^2 + hk + k^2)}{a^2} + \frac{l^2}{c^2} \right]^{\frac{1}{2}} \quad (1)$$

The estimated lattice parameters 'a' and 'c', c/a and volume are presented in Table 1. X-ray diffraction patterns of the  $\text{Cd}_{1-x}\text{Pb}_x\text{S}$  thin film are shown in Figure 1. The Table 1 reveals that the average c/a ratio is close to 1.626. The value of 'a' slightly increases and the value of 'c' decreases. These results imply that the  $\text{Pb}^{2+}$  has been substituted into the crystal lattice of CdS. As the ionic radius of  $\text{Pb}^{2+}$  (1.18  $\text{\AA}$ ) is larger than that of  $\text{Cd}^{2+}$  (0.97  $\text{\AA}$ ), the  $\text{Pb}^{2+}$  ions have been substituted into the crystal lattice of CdS and caused distortion in CdS lattice. The estimated lattice parameters are very close to the standard value. The synthesised films have wurtzite hexagonal structure. The grain size of the prepared film was estimated for the strongest peak (002) using Scherrer formula (2)

$$D_g = \frac{0.9\lambda}{\Delta \cos \theta} \quad (2)$$

$D_g$  is the average grain size,  $\lambda$  denotes the wavelength of the radiation used as the primary beam of  $\text{K}\alpha$  ( $\lambda=1.54178 \text{\AA}$ ),  $\theta$  is the angle of incidence in degree and  $\Delta$  denotes the full width at half maximum (FWHM) of the peak in radian, which was determined experimentally defined after the correction of instrumental broadening (it is  $0.05^\circ$  in the present case). The average grain size of films lies between 4 nm and 9 nm indicating the nanometric size of CdS grains developed in the film.

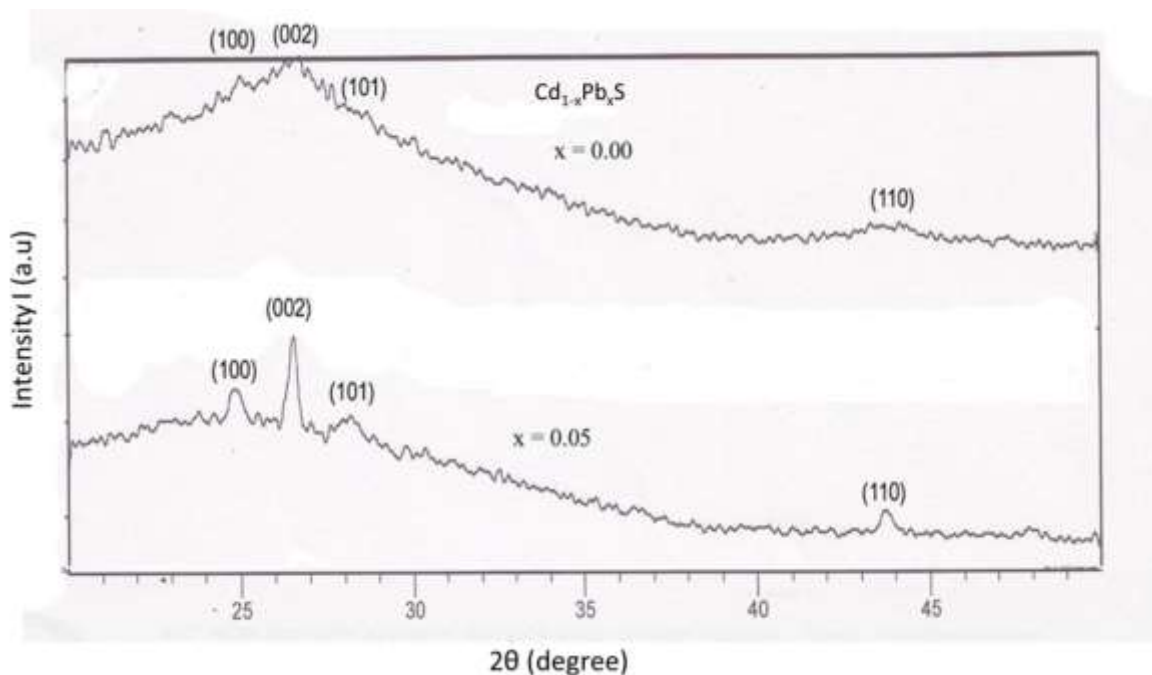
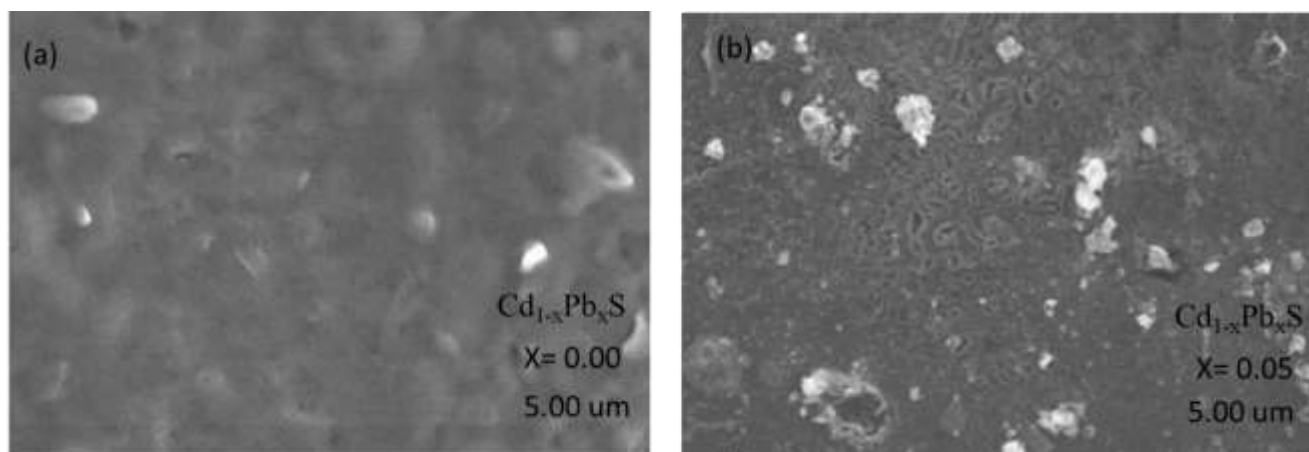


Figure 1 X-ray diffraction patterns of the  $\text{Cd}_{1-x}\text{Pb}_x\text{S}$  thin films.

Table 1 Lattice constants,  $c/a$  ratio and volume of  $Cd_{1-x}Pb_xS$  thin films

Doping concentrations, X	Lattice constants		$c/a$ ratio	Volume of CdS ( $\text{\AA}^3$ )
	A ( $\text{\AA}$ )	C ( $\text{\AA}$ )		
X=0.00	4.125	6.720	1.629	99.022
X=0.05	4.127	6.718	1.627	99.089

Energy dispersive x-ray analysis (EDX) of the films is shown in Figure 2. **Error! Reference source not found.** There is atomic percentage of Cd and S for  $x=0.00$  that confirms the CdS, film but there are values of Cd, S and Pb for  $x=0.05$ . The deposited films are  $Cd_{1-x}Pb_xS$ . The atomic percentage of Cd decreases when increasing Pb concentrations increase (Figure 3), indicating the incorporation of Pb into the system. The Figure 3 shows that Cd, S and Pb are present but the films are non-stoichiometric in composition. EDX analysis shows that the films are cadmium rich (Figure 3). This may occur because the reactivity of cadmium is greater than sulphur and lead ions. Scanning Electron Microscope (SEM) micrographs under 10000 magnification of the films are shown in Figure 2 (a) and Figure 2 (b). The films are polycrystalline in nature and deposition covers the substrate well. It also exhibits that the cluster formation in the film increases with Pb doping concentration and temperature. For pure CdS there is no precipitation of Pb, but for  $x=0.05$ , precipitation of Pb is observed in Figure 3 (a) and Figure 3 (b).

Figure 2 SEM micrograph of  $Cd_{1-x}Pb_xS$ , where  $x = 0.00$  as deposited film (0.1M) at  $300^{\circ}\text{C}$  for 10min.

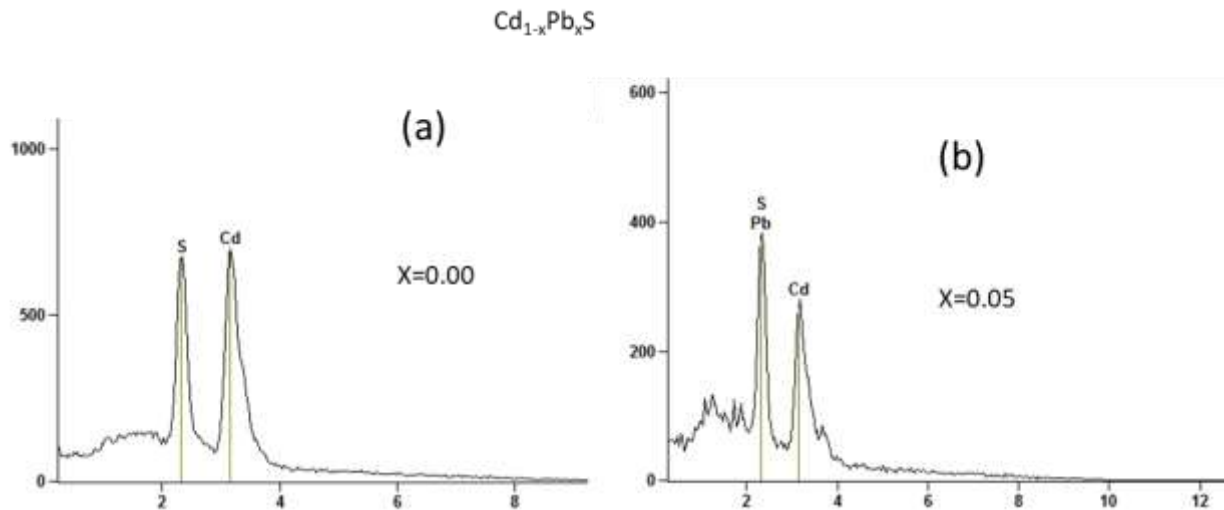


Figure 3 EDX spectrum of a  $Cd_{1-x}Pb_xS$ ,  $x=0.00$ , thin films.

### 3.2. Optical Properties

The optical properties of the films were investigated within the wavelength range 380 nm to 1100 nm which has illustrated the interaction between photon energies and films structure or among energy configurations. The optical absorption spectra of these films were taken to evaluate the absorption coefficient ( $\alpha$ ), band gap energy ( $E_g$ ) and nature of transition involved.

Figure 4 shows the wavelength dependence of the absorption coefficient of the films.

Figure 4 reveals that the optical absorption coefficient ( $\alpha$ ), is greater than  $105 \text{ cm}^{-1}$  for all the films. Also this value increases with Pb doping concentration. This may occur because the films involve several defects. The theory of optical absorption demonstrate the relationship between the absorption coefficient ( $\alpha$ ) and the photon energy ( $h\nu$ ) as

$$\alpha h\nu = A (h\nu - E_g)^n \quad 3$$

$\alpha$  denotes the absorption coefficient,  $h\nu$  denotes the photon energy,  $E_g$  denotes the optical band gap and A is the constant which is related to the effective masses associated with the valance band and the conduction band. The factor n assumes values of 1/2, 2, 3/2 and 3 for allowed direct, allowed indirect, forbidden direct, and forbidden indirect transitions, respectively. For the allowed direct type of transitions

$$\alpha h\nu = A (h\nu - E_g)^{1/2} \quad 4$$

The modes of optical transition in these films have been analyzed as shown in Figure 5.

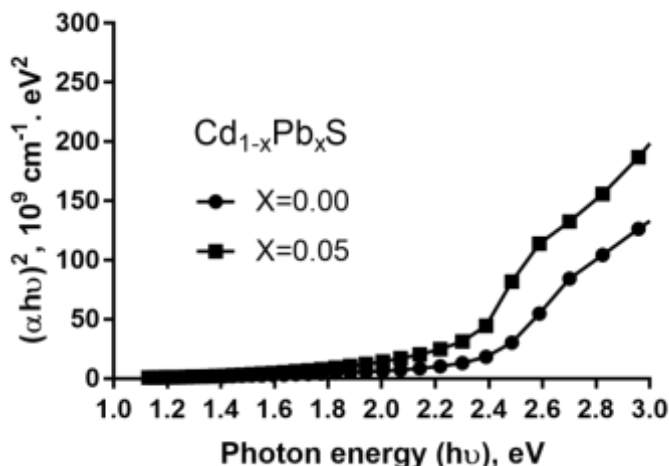


Figure 4 Variation of band gap with photon energy for Cd<sub>1-x</sub>Pb<sub>x</sub>S thin films.

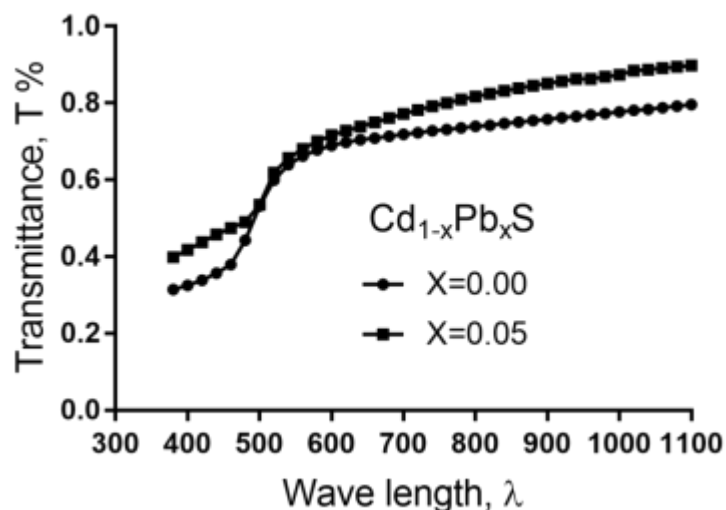


Figure 5 Variation of optical transmittance with wavelength of Cd<sub>1-x</sub>Pb<sub>x</sub>S films.

The optical band gap of pure CdS is 2.39 eV and decreases to 2.20 eV as the composition parameter 'x' increased from 0 to 0.05 which indicating that a small amount of Pb incorporation affects the optical band gap. This variation of the band gap energy benefit in designing a suitable window material in fabrication for solar cells.

#### 4. Conclusions

The films are polycrystalline in nature with wurtzite hexagonal structure and the grain sizes varied from 4 nm to 9 nm. X-ray diffraction patterns of the films are identified as (100), (002), (101), (102), (110), (103) and (201) planes. No extra peak developing with the increasing Pd concentration. The optical studies showed that the absorption coefficient ( $\alpha$ ), is very high (105 cm<sup>-1</sup>). The direct band gap energy of the films is dependent on the concentration (x). This value varies from 2.52 eV to 2.17 eV as required for solar cell and opto-electronic device applications.

## Acknowledgements

The author would like to thank Department of Physics, Faculty of Engineering, Bangladesh University of Engineering and Technology (BUET), Dhaka 1000, Bangladesh. He also extends sincere thanks BAECD for performing XRD and BCSIR for SEM & EDX measurements.

## References

1. Kamruzzaman, M., R. Dutta, and J. Podder, Synthesis and characterization of the as-deposited Cd<sub>1-x</sub>Pb<sub>x</sub>S thin films prepared by spray pyrolysis technique. *Semiconductors*, 2012. 46(7): p. 957-961.
2. Guire, M.R.D., et al., Chemical Bath Deposition, in *Chemical Solution Deposition of Functional Oxide Thin Films*, T. Schneller, et al., Editors. 2013, Springer Vienna: Vienna. p. 319-339.
3. Hop, X., et al., Growth of CdS thin films by chemical bath deposition technique. 2019.
4. Li, J., Preparation and properties of CdS thin films deposited by chemical bath deposition. *Ceramics International*, 2015. 41: p. S376-S380.
5. Saravanakumar, S., et al., Studies on Dilute Magnetic Semiconducting Co-Doped CdS Thin Films Prepared by Chemical Bath Deposition method. *Journal of Materials Science: Materials in Electronics*, 2017. 28(16): p. 12092-12099.
6. Salamon, F., Effect some Factors on the Structural Properties of the CdS Thin Films Prepared by Chemical Bath Deposition. *International Letters of Chemistry, Physics and Astronomy*, 2016. 64: p. 1-10.
7. Gaponik, N. and A.L. Rogach, Aqueous synthesis of semiconductor nanocrystals, in *Semiconductor Nanocrystal Quantum Dots: Synthesis, Assembly, Spectroscopy and Applications*, A.L. Rogach, Editor. 2008, Springer Vienna: Vienna. p. 73-99.
8. Arshad, A., et al., Aqueous synthesis of tunable fluorescent, semiconductor CuInS<sub>2</sub> quantum dots for bioimaging. *Arabian Journal of Chemistry*, 2016.
9. Dalas, E., et al., Cadmium sulfide precipitation in aqueous media: Spontaneous precipitation and controlled overgrowth on polyaniline. *Journal of Colloid and Interface Science*, 1991. 141(1): p. 137-145.
10. Singh, V. and P. Chauhan, Structural and optical characterization of CdS nanoparticles prepared by chemical precipitation method. *Journal of Physics and Chemistry of Solids*, 2009. 70(7): p. 1074-1079.
11. Butwong, N., et al., Determination of arsenic based on quenching of CdS quantum dots fluorescence using the gas-diffusion flow injection method. *Talanta*, 2011. 85(2): p. 1063-1069.
12. Polivtseva, S., et al., Spray Pyrolysis Deposition of Sn<sub>x</sub>S<sub>y</sub> Thin Films. *Energy Procedia*, 2014. 60: p. 156-165.
13. Mahmood, W., et al., Optical and electrical studies of CdS thin films with thickness variation. *Optik*, 2018. 158: p. 1558-1566.
14. Margoni, M.M., et al., Modification on the properties of vanadium oxide films deposited from NH<sub>4</sub>F added HNO<sub>3</sub> treated ammonium metavanadate precursor solution by spray pyrolysis technique. *Thin Solid Films*, 2018. 655: p. 62-69.

15. Mata, V., A. Maldonado, and M. de la Luz Olvera, Deposition of ZnO thin films by ultrasonic spray pyrolysis technique. Effect of the milling speed and time and its application in photocatalysis. *Materials Science in Semiconductor Processing*, 2018. 75: p. 288-295.
16. Moumen, A., et al., Preparation and characterization of nanostructured CuO thin films using spray pyrolysis technique. *Superlattices and Microstructures*, 2018.